Modeling one-dimensional laminar, reacting flows with an operator-splitting algorithm

J.C. Prince Avelino

Departamento de Metal-Mecánica, Instituto Tecnológico de Veracruz,
Apartado postal 3-35, 91851 Veracruz, Ver., Mexico

The purpose of the present work is to investigate an operator splitting algorithm called PISO [2, 5, 6] with respect to its suitability for transient simulations of one-dimensional, laminar combustion problems that involve multireaction chemical kinetics. To this end, in the present research the equations governing one-dimensional, laminar chemically reacting flow are formulated and relevant nondimensional parameters are determined. The governing equations are discretized using a finite-volume approach, and the PISO algorithm is implemented. Numerical solutions obtained with this algorithm are presented for a burner-stabilized, premixed ozone flame.

Keywords: Modeling, reacting flows, non-iterative algorithm, finite volume approach

El propósito del presente trabajo es investigar un algoritmo de operador separado denominado PISO [2, 5, 6] con respecto a su aplicabilidad para la simulación de problemas de combustión unidimensionales laminares que involucran cinética química de multireacciones. Para este propósito, en la presente investigación, las ecuaciones que gobiernan el flujo químicamente reactante, laminar, unidimensional son formuladas y los parámetros relevantes adimensionales son determinados. Las ecuaciones gobernantes son discretizadas usando el método de los volúmenes finitos y el algoritmo PISO es formulado. Se presentan soluciones numéricas con este algoritmo para una flama premezclada de ozono estabilizada al quemador.

Descriptores: Simulación, flujos reactantes, algoritmo no interactivo, aproximación de volumen finito

PACS: 47.70.Fw

1. Introduction

While the numerical solution of steady, one-dimensional, laminar combustion problems has become a computational task, there is a considerable lack of numerical methods that are able to accurately and efficiently solve unsteady problems. In fact, because nature is multi-dimensional and instationary, transient problems appear to be of greater relevance than their steady-state counterparts. Examples of important transient combustion problems yet awaiting numerical solution include the variety of stability problems found in nearly all engineering applications.

Different algorithms have been developed to solve the inherent complexity of the equations governing fluids flow. Explicit schemes like the FCT algorithm was specifically invented to handle problems with shock waves and it has been particularly used in high-speed reactive flow calculations [3]. In the Godunov method, a Rieman problem is solved cell by cell or region by region in the flow and integration is performed analytically extrapolating the flow forward in time. This method has been employed for shock-wave problems. Implicit finite-difference schemes are becoming favored in relation to their explicit counterparts. This is because the unconditional stability of the former as contrasted with the stability of the explicit methods which is restricted on the size of the time-step that can be taken. Existing implicit methods like SIMPLE and SIMPLER [4] methods, overcome the problem of the linkage between pressure and density for low

Mach number flows by treating the pressure as a main variable. In order to determine the pressure, a joint manipulation of the momentum and continuity equation provides an equation for the pressure. The resulting equation replaces the continuity relation while the momentum equations retain their role of determining the velocity field. The equations are discretised fully implicitly, with the pressure-velocity coupling being handled through the use of iteration. The advantage gained by implicit differencing of the equations can be diminished by the use of the iteration at each time-step which makes time-dependent calculations rather expensive. The algorithm called PISO [2] is a non-iterative method for handling the pressure-velocity coupling of the discretised momentum and pressure equations such that the fields obtained at each time-step Δt are close approximations of the exact solution of the difference equations with a formal order of accuracy of the order of powers of Δt depending on the number of operation-splittings used. This algorithm has been tested by Issa *et al.* [6] for flames where mechanisms of reaction have been linearized.

The objetive in this paper is similar to that of Heimerl *et al.* [1] and Issa *et al.* [6]; however here we make use of a laminar flame model which includes both multispecies with multireaction chemical kinetics and the momentum equation. This approach offers the advantage of complete information about the system, particularly with the highly nonlinear coupling of the energy and species equations with the fluid dynamics of the system.

2. Gasphase model

2.1. The governing equations in dimensional form

The physical problem to be analyzed is the following. A fuel-oxidizer premixture discharges from a cooled porous plug flameholder and reacts at a flame region located at a finite distance downstream of the burner exit. The burner is idealized such that the flowfield is one-dimensional, while the flame, which constitutes the reaction region, is planar and parallel to the burner exit. Assuming high activation energy of this oxidation reaction, the reaction zone is thin compared to the diffusion length of the flow. The space outside the burner is assumed to be adiabatic so that the flame loses heat only on the burner surface. In contrast to the common combustion assumption of uniform pressure, the present analysis retains the full momentum equation. The equations governing a planar, one-dimensional, laminar reactive pipe flow of an ideal-gas mixture are derived from the general conservation equations for multicomponent, reacting flows. In terms of the accumulative-convective operator L defined by

$$L(\phi) = \frac{\partial \phi}{\partial t} + u \frac{\partial \phi}{\partial x}, \tag{1}$$

for any dependent variable ϕ,* the flow field is described by the overall-continuity equation

$$L(\rho) = -\rho \frac{\partial u}{\partial x}, \tag{2}$$

and the momentum equation

$$\rho L(u) = -\frac{\partial p}{\partial x} + \frac{4}{3} \frac{\partial}{\partial x} \left(\mu \frac{\partial u}{\partial x} \right). \tag{3}$$

Temperature and mass fractions obey the energy and species conservation equations, respectively, *viz.*,

$$c_p \rho L(T) = \frac{\partial}{\partial x} (\lambda \frac{\partial T}{\partial x}) + L(p) - \sum_{i=1}^{N} h_i w_i, \tag{4}$$

$$\rho L(Y_i) = -\frac{\partial}{\partial x} (\rho Y_i V_i) + w_i, \quad i = 1, \dots, N. \tag{5}$$

We refer to *e.g.* Williams [8] for the derivation of these equations, which rely on classical assumptions such as Fourier law, Fick's law, Arrhenius law, the law of mass action and the perfect gas equation of state, and where the external forces are neglected. In Eqs. (1) to (5), and below, t denotes the time, x the spatial coordinate, and u the velocity component in the x direction; ρ is the density, p is the pressure, T the temperature and Y_i the mass fraction of species i, $i = 1, \dots, N$. μ denotes the dynamic viscosity of the mixture, λ its thermal conductivity and c_p its specific heat capacity at constant pressure; h_i is the specific enthalpy of species i, $i = 1, \dots, N$, V_i its diffusion velocity and w_i its mass rate production. The system of Eqs. (2) to (5) is closed by the ideal-gas equation of state:

$$\rho = p\gamma,$$

where

$$\gamma = \left[R^0 T \sum_{i=1}^{N} \left(\frac{Y_i}{W_i} \right) \right]^{-1}. \tag{6}$$

Here R^0 denotes the universal gas constant and W_i, the molecular weight of species i, $i = 1, \dots, N$.

2.2. Initial and Boundary conditions

The governing equations, Eqs. (2) to (5) form a hybrid parabolic-hyperbolic system of partial differential equations. In only a few special cases the mathematical formulation of the boundary conditions, which are to be imposed to ensure existence and uniqueness of the solution, are known. Therefore, it is necessary that proper boundary conditions are chosen in a heuristic way by taking into account the physical meaning of the combustion problem under consideration and the mathematical nature of the governing equations.

With the burner exit as the origin, the boundary conditions are given by[†]

$$x = 0: \quad T = T_u, \quad Y_i = Y_{i,u},$$
$$i = 1, \dots, N \quad \text{and} \quad u = u_u; \tag{7}$$

$$x \to \infty: \quad \frac{\partial T}{\partial x} = \frac{\partial Y_i}{\partial x} = 0,$$
$$i = 1, \dots, N \quad \text{and} \quad \frac{\partial u}{\partial x} = 0, \quad p = p_c. \tag{8}$$

The subscript u identifies properties in the unburnt gas. These conditions imply that the flow temperature and discharge rate are fixed at the burner exit, that there is no species penetration into the burner, and that all properties are bounded far downstream of the flame where the fuel concentration vanishes because of a complete oxidation reaction. For the fluid dynamics system, at $x = 0$, the velocity is prescribed (discharge rate fixed), while the pressure there is computed from the momentum equation. At the postflame boundary, the pressure is fixed to be p_c, while the velocity there is updated by setting zero gradient to the velocity. The model was started from a standard initial profile (see Fig. 1) and ended the exercise at a time to ensure that steady state had been achieved.

2.3. Model for thermodynamics and molecular transport

Following [3], it is assumed that the diffusion velocity can be written as

$$V_i = V_i^D + V_i^T + V_c. \tag{9}$$

In Eq. (9) V_i^D is the ordinary-diffusion velocity, V_i^T is the thermal diffusion velocity and V_c is the correction velocity.

The dynamic viscosity and the thermal conductivity of the mixture are calculated from the respective properties of the pure species according to the widely accepted approxima-
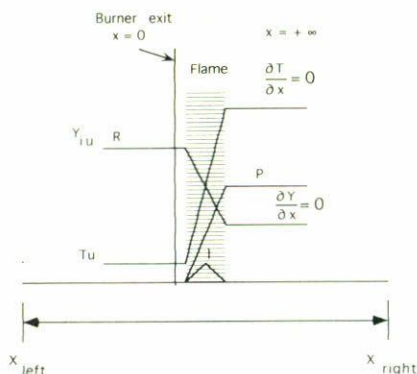
FIGURE 1. Schematic diagram of boundary conditions. Also, the initial profiles to be specified to start from scratch the computation of a burner-stabilized premixed flame, R and P are the rectants and products, respectively.

tions

$$\mu = \frac{1}{2}\left(\sum_{i=1}^{N} X_i \mu_i + \frac{1}{\sum_{i=1}^{N} X_i/\mu_i}\right), \tag{10}$$

and

$$\lambda = \frac{1}{2}\left(\sum_{i=1}^{N} X_i \lambda_i + \frac{1}{\sum_{i=1}^{N} X_i/\lambda_i}\right). \tag{11}$$

Here X_i denotes the mole fraction of species i. For the thermodynamic properties polynomial curve fits of the NASA type are used. Thus, the molar specific heat capacity at constant pressure is given by

$$\frac{C_{pi}}{R^0} = a_1 + a_2 T + a_3 T^2 + a_4 T^3 + a_5 T^4, \tag{12}$$

the molar specific enthalpy by

$$\frac{H_i}{R^0} = a_6 + a_1 T + \frac{a_2}{2}T^2 + \frac{a_3}{3}T^3 + \frac{a_4}{4}T^4 + \frac{a_5}{5}T^5, \tag{13}$$

and the molar specific entropy by

$$\frac{S_i}{R^0} = a_7 + a_1 \ln T + a_2 T + \frac{a_3}{2}T^2 + \frac{a_4}{3}T^3 + \frac{a_5}{4}T^4. \tag{14}$$

2.4. Model for combustion chemistry

When detailed mechanisms of elementary reactions are employed in the numerical simulation of laminar flames, the rates of production of the chemical species may be written as

$$w_i = W_i \sum_{k=1}^{M}(\nu_{i,k}'' - \nu_{i,k}')(AT^\alpha)_k \exp\left(-\frac{E_k}{R^0 T}\right)$$

$$\times \prod_{j=1}^{N}\left(\frac{\rho Y_j}{W_j}\right)^{\nu_{j,k}'}, \quad i = 1, \dots, N, \tag{15}$$

where it is understood that forward and backward chemical reactions are treated separately. Besides the quantities already

defined above, in Eq. (15) M denotes the number of elementary reactions contained in the mechanism, and $\nu_{j,k}'$ and $\nu_{j,k}''$ are the stoichiometric coefficients of species i in reaction k, $k = 1, \dots, M$, representing there reactants and products, respectively; (AT^α) y E_k are the pre-exponential factor in the specific reaction-rate constant and the activation energy of reaction k, respectively.

2.4.1. The ozone kinetic mechanism

We have studied the ozone flame because its kinetic mechanism is the simplest existing detailed mechanism of elementary reactions. It involves three species, O, O_2 and O_3 which react according to the mechanism shown below

$$O_3 + M \rightleftharpoons O + O_2 + M,$$

$$O + O_3 \rightleftharpoons 2O_2, \tag{16}$$

$$2O + M \rightleftharpoons O_2 + M,$$
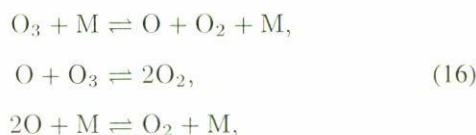
where M represents a third body, which can be either O, O_2, or O_3.

3. Numerical method

3.1. The governing equations in nondimensional form

Nondimensional numbers that can be formed by introducing or selecting, respectively, reference quantities are the Strouhal number Sr, the Reynolds number Re, the Euler number Eu, the Prandtl number Pr, and the Mach number Ma. In terms of the quantities defined above, the nondimensional governing equations can be written as

$$L^\star(\rho^\star) = -\rho^\star \frac{\partial u^\star}{\partial x^\star}, \tag{17}$$

$$\rho^\star L^\star(u^\star) = -Eu\frac{\partial p^\star}{\partial x^\star} + \frac{4}{3Re}\frac{\partial}{\partial x^\star}\left(\mu^\star \frac{\partial u^\star}{\partial x^\star}\right), \tag{18}$$

$$c_p^\star \rho^\star L^\star(T^\star) = \frac{1}{RePr}\frac{\partial}{\partial x^\star}\left(\lambda^\star \frac{\partial T^\star}{\partial x^\star}\right)$$

$$+ (\kappa - 1)Ma^2 EuL^\star(p^\star) - \sum_{i=1}^{N} h_i^\star w_i^\star, \tag{19}$$

$$\rho^\star L^\star(Y_i^\star) = -\frac{\partial}{\partial x^\star}(\rho^\star Y_i^\star V_i^\star) + w_i^\star, \quad i = 1, \dots, N. \tag{20}$$

where the nondimensional operator $L^\star$ is given by

$$L^\star(\phi^\star) = Sr\frac{\partial \phi^\star}{\partial t^\star} + u^\star \frac{\partial \phi^\star}{\partial x^\star}. \tag{21}$$

Here, κ is the ratio of reference specific heat capacities. The nondimensional equation of state is

$$\rho^\star = Ma^2 Eu(p^\star + q^\star)\gamma^\star,$$

where

$$\gamma^\star = \left[T^\star \sum_{i=1}^{N}\left(\frac{Y_i}{W_i/W_{\text{ref}}}\right)\right]^{-1}. \tag{22}$$

3.2. Discretization

For convenience of notation subsequently the superscript indicating nondimensional quantities ($\star$) will be omitted. For the derivation of difference equations it is convenient to write each of the governing equations in a standard form consisting of an accumulative term , a convective term, a diffusive term and a source term, *viz.*,

$$Sr\frac{\partial(\rho\phi)}{\partial t} + \frac{\partial(\rho u\phi)}{\partial x} = \frac{\partial}{\partial x}\left(\Gamma_\phi\frac{\partial\phi}{\partial x}\right) + S_\phi. \qquad (23)$$

Here ϕ is unity for the continuity equation, u for the momentum equation, T for the energy equation, and Y_i for the i-th species-mass conservation equation, $i = 1, \ldots, N$. The general procedure to cast a partial differential equation into the above standard form is to manipulate the equation until all coefficients and terms appearing in it are in a form suitable to be absorbed into the "generalized diffusion coefficient" Γ_ϕ and the source term S_ϕ.

The method selected herein to derive difference equations from the governing partial differential equations, Eqs. (17)–(20), is the finite-volume method (FVM). The essence of the FVM consists of defining for each point P of the computational domain a suitable control volume surrounding that point, and to integrate the governing equation of the respective dependent variable over the control volume, see Fig. 2. The control volumes are selected such that, firstly, each volume surrounds one and only one grid point, secondly, that the control volumes do not overlap, and thirdly, that their collection covers the total volume under consideration. The result of the integration over a control volume surrounding grid point P is a difference equation, the unknowns in which are the values of the dependent variables at point P and at the western and eastern neighbors of P.

Upon integration of Eq. (23) over a computational grid point P, illustrated in Fig. 2, and after some algebraic manipulations, the discretised equation may be written as

$$\phi_P(\beta\rho - A)_P = H_P(\phi) + \overline{S}_{\phi,P} + \beta_P(\rho\phi)_P^n, \qquad (24)$$

where $\overline{S}_{\phi,P}$ denotes the volume integral over the source term S_ϕ. In Eq. (24) and below the superscript n is used to identify variables or expressions taken at time level $t \equiv t^n$ at which a solution to the governing equations is assumed to be known. Variables or expressions not identified by the superscript n are to be taken at time $t = t^n + \Delta t$ and are unknown; solutions to the governing equations at time $t = t^n + \Delta t$ are sought. The individual terms of Eq. (24) are given by

$$\beta_P = \frac{Sr\delta x_P}{\Delta t}, \qquad (25)$$

$$-A_P = (\alpha M)_e + (\alpha M)_w - M_w, \qquad (26)$$

$$H_P(\phi) = (\alpha M)_e\phi_E + (\alpha M)_w\phi_W, \qquad (27)$$
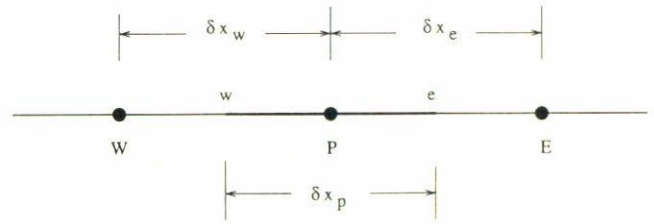
FIGURE 2. Labeling of grid points and boundary points of a control volume surrounding point P. The width of the control volume is δx_P; both its height δy_P and its depth δz_P are one. Point P is located in a cuboid control volume δV_P; its neighboring grid points are W and E. The boundaries of the control volume surrounding P are labeled w and e.

where $M = \rho u$ is the mass flux and the parameter α_i is defined as

$$\alpha_i = \begin{cases} \frac{1}{2}(1 + 2/Pe_i) & \text{for } |Pe_i| \leq 2, \\ 1 & \text{for } Pe_i > 2, \\ 1 & \text{for } Pe_i < -2. \end{cases} \qquad (28)$$

Here central and upwind formulations are represented. The values zero ore one for α_i denote those cases where diffusive transport is neglected compared to convection. Pe is the Peclet number ($Pe = \rho u\delta x/\Gamma_\phi$).

3.2.1. Staggered grid for the momentum equation

Shown in Fig. 3 is a control volume in the staggered grid of the velocity u, which is assumed to be governed by the momentum Eq. (18). It is seemed from Figs. 2 and 3 that the staggered grid for u can be obtained from the basic grid by shifting the center of mass of each basic-grid control volume V_P a distance $\frac{1}{2}(x_E - x_P)$ to the right. Thus, for the staggered u grid, the momentum equation becomes

$$\phi_P(\beta\rho - A)_e = H_e(\phi) - Eu(p_E - p_P)$$
$$+ \overline{S}_{\phi,e} + \beta_e(\rho\phi)_e^n, \qquad (29)$$

where β_e, A_e, H_e, and α_e are defined in a similar way as in Eqs. (25)–(28).

3.3. The PISO algorithm

Now we briefly describe the revised PISO algorithm [6] and its numerical implementation. The algorithm consists of a series of steps, one predictor and two correctors, that are to be carried out during each time-step. For convenience of presentation, the equations are written in the general form

$$B\phi = C_P(\phi) + S_P(\phi) + G\phi_P^n. \qquad (30)$$

where B denotes the sum of all coefficients of the variable ϕ at point P; C_P is a function of terms coupling ϕ_P to the neighbours ϕ_E and ϕ_W; S_P is the sum of the source terms of
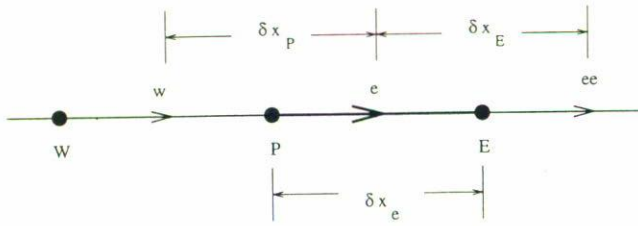
FIGURE 3. Staggered grid for the velocity u.

ϕ_P; and G denotes the coefficient of ϕ_P^n, *i.e.*, the value of the variable ϕ at the previous time level t^n.

Predictor step. For all dependent variables, the values prevailing at time level t^n are used in the solution of the momentum Eq. (29) and scalar (energy and mass fractions) Eqs. (24). The coefficients in the operators A and H are evaluated at time t^n so that, these operators are linear with respect to u. Also the source terms are evaluated at t^n. Thus, at each interior grid location P, the linear problems

$$B_P^n \psi_P^\star = C_P^n(\psi^\star) + \overline{S_{\psi,P}^{\prime n}} + G\psi_P^n, \tag{31}$$

are solved for the starred variable $\psi^\star$. Note that in general the starred velocity field does not satisfy the continuity equation.

First corrector step. Here, the coefficients A and H are still evaluated at the old time level. Continuity, momentum and state equations are used to derive the pressure equation

$$B_P^n p_P^\star = C_P^n(p^\star) + \overline{S_{p,P}^{\prime n}} + G p_P^n, \tag{32}$$

and is solved for $p^\star$. The new pressure $p^\star$ is subsequently used in solving the density field

$$\rho^\star = EuMa^2(p^\star + q)\gamma^\star. \tag{33}$$

The double-starred velocity field is obtained by solving the correspondingly Eq. (29). The velocity field $u^{\star\star}$ and the density field $\rho^\star$ which now satisfy the continuity equation are used to update the coefficients $A_{\phi P}$ and $H_{\phi P}$ in Eq. (24). Thus, the scalar equations

$$B_P^n \phi_P^{\star\star} = C_P^n(\phi^\star) + \overline{S_{\phi,P}^{\prime n}} + G\phi_P^n, \tag{34}$$

are explicitly solved for $\phi^{\star\star}$.

Second corrector step. Firstly, the continuity-based pressure equation

$$B_P^n p_P^{\star\star} = C_P^n(p^{\star\star}) + \overline{S_{p,P}^{\prime n}} + G p_P^n, \tag{35}$$

is solved. Then, the new double-starred pressure is subsequently used in solving the density field

$$\rho^{\star\star} = EuMa^2(p^{\star\star} + q)\gamma(T^{\star\star}). \tag{36}$$

The triple-starred velocity field is obtained by solving the correspondingly Eq. (29). The velocity field $u^{\star\star\star}$ and the density

field $\rho^{\star\star}$ which now satisfy the continuity equation are used to update the coefficients $A_{\phi P}$ and $H_{\phi P}$ in Eq. (24). Thus, the scalar equations

$$B_P^n \phi_P^{\star\star\star} = C_P^n(\phi^{\star\star\star}) + \overline{S_{\phi,P}^{\prime n}} + G\phi_P^n, \tag{37}$$

are explicitly solved for $\phi^{\star\star\star}$.

4. Results and discussions

4.1. Computational procedure

To perform the simulation of a steady, laminar, burner-stabilized ozone flame, the PISO algorithm was implemented into the Universal Laminar Flame and Flamelet Code RUN-1DL [7], which provides the facilities required for the simulation of reacting and non-reacting quasi-one-dimensional flows with detailed models of chemistry, thermodynamics and molecular transport. Adaptive griding can be employed with this code.

To start the simulation of the flame, guessed initial profiles of the dependent variables are required (Fig. 1). The initial guess calculated internally by RUN-1DL [7] is taken by the PISO algorithm, which then is used for as many time-steps as are required to reach a steady solution.[‡] One of the main problems during this simulation was the occasional movement of the flame out of the computational domain. This problem was eliminated by using adaptive griding implemented in RUN-1DL. A time-step size of 10^{-7} seconds was used.

4.2. Interpretation of profiles

For the burner-stabilized premixed flame calculated herein, a temperature of 300 K was adopted at cold boundary where the species were assumed to contain fixed mass fractions of O_3 (60 %) and O_2 (40 %). The specified burning velocity at the cold boundary was 1.5 m/s, while the pressure in the hot boundary is fixed to be 1 bar.

Shown in Fig. 4 are the results of the steady solution of the burner-stabilized ozone flame. In the left-hand part of the picture the temperature, velocity and pressure profiles through the flame are shown, while in the right-hand part the mass fraction of the species are plotted. It can be seen from the figures that due to the large activation energy reaction the ozone flame structure consists of a thin chemically-reacting region (0.2 mm in physical space)[**] separating two broad, upstream unburnt and downstream burnt regions in which fuel oxidation effectively does not occur. In this thin region convection is unimportant such that the controlling processes are diffusion, oxidation, dissociation and recombination. On the postflame region, the temperature, velocity and mass fraction profiles generated by the model tend to constant values (zero gradients), correspondingly to the boundary conditions.

The temperature graph displays a steep slope near the cold boundary, while in the postflame region there is a slow
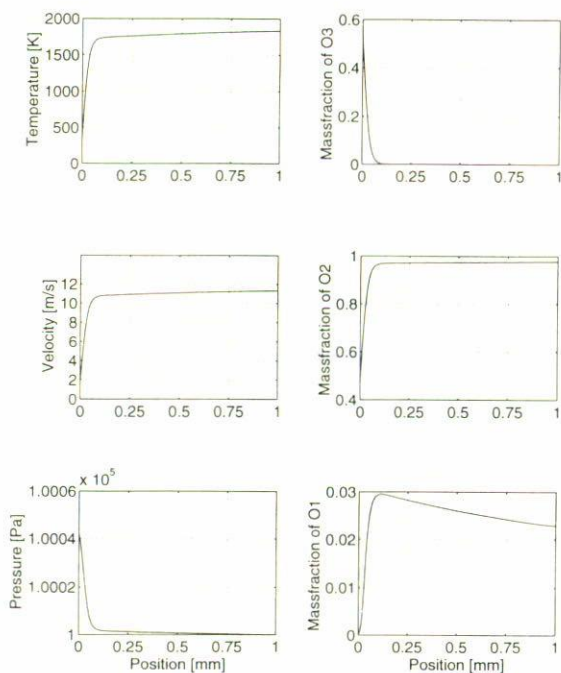
FIGURE 4. Profiles through a laminar burner-stabilized ozone flame.

temperature rise with a maximum temperature of 1900 K. The mass fractions profiles depicted herein show that the structure for the ozone flame occurs in the hot reaction zone and the O atoms produced there diffuse into the preheat zone, where the exotermic step occurs, converting the preheat zone

into an exothermic zone. The gas velocity profile shows how the unburned gases move at the specified burning velocity of 1.5 m/s through the flame region where the velocity increases sharply, while in the postflame region the velocity tends to a constant value. As it is to be expected on physical grounds, a negligible pressure drop occurs in the flame. Therefore, the common assumption of constant pressure across a flame used in other steady-state calculations is satisfied. It can be seen from this figure that an almost perpendicular gradient develops over the flame region, while in the postflame region the slope gradually decreases to approach the specified pressure of 1 bar.

5. Concluding remarks

The present work investigates the PISO algorithm with respect to its suitability for simulations of one-dimensional laminar premixed flames with detailed chemistry model for the flame. To this end, the equations governing one-dimensional, laminar chemically reacting flows are nondimensionalized and discretised using a finite volume approach, and the PISO algorithm is implemented into a computational code. A burner-stabilized ozone flame with detailed chemistry was used to test the capability of the code for handling the nonlinear coupling of the energy and species equations with the fluid dynamics of the system. It was shown that this model predicts pressure drops that are in resonable agreement to the physical problem.

---

*. The quantity $L(\phi)$ is the total derivative of ϕ.

†. A schematic diagram of the initial and boundary conditions on a burner is shown in Fig. 1.

‡. Only the final steady solutions resulting from this exercise are presented for clarity.

**. As a consequence, the adaptive gridding is necessary.

1. J.M. Heimerl and T.P. Coffe, *Combustion and Flame* **39** (1980) 301.

2. R.I. Issa, *J. Comp. Phys.* **62** (1986) 40.

3. E.S. Oran and J.P. Boris, *Progress in Energy and Combustion Science* **39** (1981) 1.

4. S.V. Patankar, *Numerical Heat Transfer and Fluid Flow*, (Hemisphere Publishing Corp., New York, 1980).

5. A.D. Gosman, R.I. Issa, and A.P. Watkins, *J. Comp. Phys.* **62** (1986) 66.

6. K.R. Beshay, R.I. Issa, B. Ahmadi-Befrui, and A.D. Gosman, *J. Comp. Phys.* **93** (1991) 388.

7. B. Rogg, *Run-1dl: The universal laminar flamelet code*, Technical report, Ruhr-Universitat Bochum, Lehrstuhl fur Stromungsmechanik, Institut fur Thermo- Fluiddynamik, D-44780 Bochum, Germany, 1994.

8. F.A. Williams, *Combustion Theory*, 2nd edition (Benjamin/Cummings, 1985).